Quantitative Evaluation of Annuloplasty on Mitral Valve Chordae Tendineae Forces to Supplement Surgical Planning Model Development

Andrew W. Siefert, M.S.[a,c], **Jean-Pierre M. Rabbah, Ph.D.**[a,c], **Eric L. Pierce, B.S.**[a], **Karyn S. Kunzelman, Ph.D.**[b], and **Ajit P. Yoganathan, Ph.D.**[a,*]

[a]The Wallace H. Coulter Department of Biomedical Engineering, Georgia Institute of Technology and Emory University, Atlanta, Georgia

[b]Department of Mechanical Engineering, University of Maine, Orono, Maine

Abstract

Purpose—Computational models of the heart's mitral valve (MV) exhibit potential for preoperative surgical planning in ischemic mitral regurgitation (IMR). However challenges exist in defining boundary conditions to accurately model the function and response of the chordae tendineae to both IMR and surgical annuloplasty repair. Towards this goal, a ground-truth data set was generated by quantifying the isolated effects of IMR and mitral annuloplasty on leaflet coaptation, regurgitation, and tethering forces of the anterior strut and posterior intermediary chordae tendineae.

Methods—MVs were excised from ovine hearts (N=15) and mounted in a pulsatile heart simulator which has been demonstrated to mimic the systolic MV geometry and coaptation of healthy and chronic IMR sheep. Strut and intermediary chordae from both MV leaflets (N=4) were instrumented with force transducers. Tested conditions included a healthy control, IMR, oversized annuloplasty, true-sized annuloplasty, and undersized mitral annuloplasty. A2-P2 leaflet coaptation length, regurgitation, and chordal tethering were quantified and statistically compared across experimental conditions.

Results—IMR was successfully simulated with significant increases in MR, tethering forces for each of the chordae, and decrease in leaflet coaptation (p<.05). Compared to the IMR condition, increasing levels of downsized annuloplasty significantly reduced regurgitation, increased coaptation, reduced posteromedial papillary muscle strut chordal forces, and reduced intermediary chordal forces from the anterolateral papillary muscle (p<.05).

Conclusions—These results provide for the first time a novel comprehensive data set for refining the ability of computational MV models to simulate IMR and varying sizes of complete rigid ring annuloplasty.

Keywords

Mitral Valve; Annuloplasty; Computational Methods; Chordae Tendineae; Heart Valve; Mitral Regurgitation

[*]Corresponding Author: Ajit P. Yoganathan, 387 Technology Circle, Office 234, Atlanta, GA 30313-2412, Ph. (404) 894-2849, Fax. (404) 894-4243, ajit.yoganathan@bme.gatech.edu.
[c]Andrew W. Siefert and Jean-Pierre M. Rabbah are co-first authors.

Conflict of Interest Statement
None.

Introduction

Ischemic mitral regurgitation (IMR) occurs when the heart's mitral valve (MV) is rendered incompetent by post-infarction left ventricular remodeling and gross three-dimensional alterations in MV geometry.[8] These alterations include papillary muscle displacement and annular dilatation which ultimately lead to restricted leaflet motion and mitral regurgitation.[30] Compared to degenerative heart valve pathologies, the ischemic MV tissue structure and material properties are considered to remain relatively unchanged from a healthy state.[1,19] This unique characteristic has provided a welcomed framework for developing computational MV models and has fostered their transition to IMR surgical planning tools.

The ultimate goal of such computational tools is to predict how effective a proposed surgical strategy may be for addressing a patient's MV anatomy and dysfunction. In reaching toward this goal, several models have sought to simulate the preferred IMR surgical repair known as undersized mitral annuloplasty (UMA).[29,31,34] In this procedure, the dilated mitral annulus is constrained to the shape and size of an undersized complete rigid annuloplasty ring.[2] This ring forces the mitral leaflets into apposition to compensate for the excessive chordal-leaflet tethering caused by post-infarction ventricular dilatation.[3] While effective in the majority of patients, UMA can worsen chordal-leaflet tethering and result in postoperative recurrent mitral regurgitation (MR) (~10–15% of patients).[11,17,21] The ability of computational MV models to recreate and predict these repair induced effects would significantly contribute to improving patient-repair selection and reducing suboptimal surgical outcomes.

While significant technological advances in MV models have been made, many challenges remain for realistically modeling UMA's effects on chordal-leaflet tethering. A significant challenge is modeling the complex architecture and function of the MV's chordae tendineae. Current standard-of-care echocardiography is unable to spatially resolve the detailed chordal architecture requiring MV models to employ idealized chordal distributions.[4,18,20,24,26,29,31–33] These idealized chordal geometries can differ greatly from native valves and have been demonstrated to impact MV simulation results.[20,32] Compounding this uncertainty is the lack of experimental data providing boundary conditions for how the tethering of the chordae may change from IMR to UMA. Addressing both challenges is critical for improving IMR surgical planning tools and advancing their predictive capabilities.

One step towards improving MV modeling therefore is to define boundary conditions that describe the changes in tethering that occur with the MV's primary load bearing chordae in IMR and UMA. While select *in vitro* and large animal studies have quantified chordal forces,[25] no studies have quantified chordal tethering during the sequential transition from a healthy MV to IMR and UMA. The ability to quantify chordal forces in these conditions will therefore enhance MV model development. To this end, the aim of this study was to generate an *in vitro* ground-truth data set by quantifying the isolated effects of IMR and UMA on leaflet coaptation, MR, and tethering forces of the anterior strut and posterior intermediary chordae tendineae from both the anterolateral and posteromedial papillary muscles.

Methods

In-Vitro Simulation of Ischemic Mitral Regurgitation

In vitro simulation was conducted in the extensively studied Georgia Tech left heart simulator.[10,12,14,15,22,27,28] This closed-loop simulator allows for precise control of annular and subvalvular MV geometry at physiological left heart hemodynamics. This *in vitro* model

has been previously demonstrated to mimic the systolic MV geometry, leaflet coaptation, regurgitation, and anterior leaflet strain of a healthy and chronic IMR ovine model.[28] Within this simulator, freshly excised MVs are sutured to an adjustable annulus capable of asymmetric dilatation as well as conforming to the shape of annuloplasty rings. The annulus in the present study could conform to the shape of a size 34 (oversized), 30 (true-sized), and 26 (undersized) Physio™ annuloplasty ring (Edwards Lifesciences, Irvine, CA). The control annulus area was approximately 440 mm^2 while the IMR area was approximately 700 mm^2. The shape of the dilated annulus was constructed based on the posteromedially dilated annular geometries measured within an ovine model of chronic IMR.[7]

Within the simulator, papillary muscle (PM) positions were controlled by two mechanically adjustable positioning rods capable of achieving positions in the apical, lateral, and posterior directions at a resolution of ±0.25 mm. Transmitral flow was measured using an electromagnetic probe (Carolina Medical Electronics, FM501D, East Bend, NC) mounted upstream of the atrium. Transmitral pressure was monitored with transducers mounted in the atrium and ventricle (calibrated accuracy ± 1 mmHg) (Validyne DC-40, Northridge, CA).

Chordae Tendineae Force Transducers

Miniature c-shaped force transducers have been used previously to quantify tethering forces of the MV's chordae tendineae.[14,15,22,23] These transducers are strain gage based and manufactured, tested, and calibrated before and after each experiment within our laboratory. During calibration, the linear regression coefficient for the relationship between the calibrated load and transducer voltage output are between 0.98–1.00. The relative difference between measured and true values (accuracy) after calibration is less than 2% with a minimum measurable tension of approximately 0.01 N. Prior to each experiment, these transducers are sutured directly (using 17 mm RB-1 needle with 5-0 silk, Ethicon, Somerville, NJ) to selected strut chordae tendineae without altering the chord's native length. Once a transducer is secured to the chord, the section of chordae located between the transducer's measurement arms is transected such that all tensile loading of the chord is transferred to the transducer.

Experimental Protocol

Fifteen ovine MVs with an anterior leaflet height of 20–25 mm were utilized in this study. Anterior leaflet height has been demonstrated to correlate with commissural width and thus healthy annular area in more than 90% of cases.[5] If the selected MV was found to possess any mitral chordae that inserted directly in the LV wall, the valve was discarded and another MV was selected for experimentation. No additional screening criterion was used in mitral valve selection.

After suturing the excised MV to the simulator's mitral annulus, 4 chordae tendineae were instrumented with dedicated chordal force transducers. Selected chordae included the anterior strut and posterior intermediary chords originating from both the anterolateral and posteromedial papillary muscles. Following instrumentation, the MV was mounted into the simulator and the annulus was conformed to a size 30 Physio™ ring. Upon establishing human left heart hemodynamics (cardiac output 5.0 L/min, 70 beats/min, 120 mmHg transmitral pressure), each papillary muscle was carefully positioned and fine-tuned to establish the control MV geometry.[14] Mitral coaptation was inspected via echocardiography such that the anterior leaflet spanned approximately two-thirds of the A2-P2 diameter. When the control valve geometry conditions were successfully achieved, the experimental endpoints of transmitral flow, left atrial pressure, left ventricular pressure, 2D echocardiography (Philips ie-33 Matrix, Phillips Healthcare, Andover, MA), and chordal forces were acquired.

To simulate chronic IMR due to an inferior myocardial infarction, the valve annulus was asymmetrically dilated to approximately 150% of the control valve area.[7,28] The anterolateral papillary muscle was displaced 3 mm apically and 2 mm anteriorly, whereas the posteromedial papillary muscle was displaced 4 mm apically, 4 mm posteriorly, and 8 mm laterally. These changes were consistent with previously published data from chronic ischemic mitral regurgitation due to inferior myocardial infarction.[28,30] Papillary muscles where held in their displaced IMR positions for all levels of simulated annuloplasty (Figure 1). This was done to reflect the results of a previous porcine IMR study that demonstrated undersized Physio™ ring annuloplasty to not induce an overall pattern of PM relocation.[13] Upon establishing these conditions, all endpoints were acquired. Following the simulation of IMR, the annulus was sequentially conformed to the shape of 3 mitral annuloplasty ring sizes. These conditions included an oversized condition (size 34 Physio™ Ring), a true-sized condition (size 30 Physio™ Ring), and an undersized mitral annuloplasty condition (size 26 Physio™ Ring). These experimental conditions are sequentially shown in Figure 1. At each condition, all experimental endpoints were recorded.

Data and Statistical Analyses

All data was processed offline within a custom MATLAB program and averaged over 10 consecutive cardiac cycles. All data is expressed as a mean ± standard error. Mitral regurgitation volume was measured directly by an electromagnetic flow probe located upstream of the atrium and was calculated as the total retrograde volume occurring during MV closure. Echocardiography data were analyzed using Phillips QLab (v.7.0; Philips Healthcare; Andover, MA). Measured endpoints were checked for normality using the Anderson-Darling test. A general linear model using each valve as a random factor was used to investigate the effect of the valve and experimental condition on each of the measured endpoints. To decrease the probability of type I errors, a Bonferroni post hoc test was used to determine if significant differences in each metric existed between experimental conditions. All statistical analyses were completed using Minitab 16 (Minitab Inc, State College, PA).

Results

Mitral Regurgitation Volume

Mitral regurgitation was observed to significantly differ between experimental conditions (p<.001) (Table 1). Mean MR volumes expectedly increased from control to IMR (p<.001). At the IMR condition, each regurgitant jet was asymmetric and originated from the tethered A3-P3 leaflets. Following IMR, MR volumes were significantly reduced with increasing levels of annuloplasty ring under sizing (p<.001). While oversized annuloplasty reduced MR volumes from the IMR condition, MR volumes at oversized annuloplasty remained significantly greater than that of the control (p<.001). Elimination of MR was successfully achieved with both true-sized and undersized annuloplasty. Both of these repairs resulted in MR volumes that were not statistically different from the healthy control.

A2-P2 Leaflet Coaptation Length

Leaflet coaptation length across the 12 to 6 o'clock annular diameter was observed to significantly differ between the tested conditions (p<.001) (Table 1). The largest reduction in coaptation length was observed between the control and IMR condition (p<.001). Reshaping the mitral annulus to an oversized or true-sized ring slightly improved coaptation length but these improvements remained significantly less than the coaptation length occurring in the control condition (p<.001). Undersized annuloplasty was the only repair condition which successfully restored A2-P2 coaptation length to values not-statistically different from the healthy control condition.

Chordal Tethering from the Posteromedial Papillary Muscle

Simulating an inferior myocardial infarction resulted in significant changes in chordal tethering for the posteromedial PM's anterior strut and posterior intermediary chordae (p<.001) (Table 2). Anterior strut chordal forces were observed to approximately double with IMR (p<.01) (Figure 2). With simulated MV repair, anterior strut chordal forces were significantly reduced from the IMR condition at each level of mitral annuloplasty (p<.005). Compared to the IMR condition, undersized annuloplasty significantly reduced anterior strut chordal forces by approximately 27% (p<.001). Despite this result, anterior strut chordal forces at each level of annuloplasty remained significantly larger than forces measured in the control condition (Table 2).

Similar to the anterior strut chordae, the posterior intermediary chordal forces were observed to significantly increase with IMR (p<.001). However, no statistically significant differences were observed between the IMR condition and each level of annuloplasty (Table 2). Among the tested conditions, posterior intermediary forces remained significantly greater than those observed during the control condition (p<.001). While not statistically significant, posterior intermediary forces demonstrated an increasing trend from oversized to undersized annuloplasty (Figure 2). Following undersized annuloplasty, posterior intermediary chordal forces were only marginally reduced (by approximately 4%) from the IMR condition.

Chordal Tethering from the Anterolateral Papillary Muscle

Similar to chordae from the posteromedial PM, simulating an inferior myocardial infarction resulted in significant changes to anterior strut and posterior intermediary tethering from the anterolateral PM (p<.001). Anterior strut and posterior intermediary forces were both observed to significantly increase with IMR (p<.005). With increasing levels of annular under sizing, anterior strut chordal forces were found to significantly decrease between the IMR and undersized annuloplasty condition (p<.05). Similarly, posterior intermediary chordal forces were observed to significantly decrease from the IMR condition to true-sized (p<.05) and undersized (p<.01) annuloplasty respectively.

Chordal Tethering Forces Summed by Papillary Muscle

The strut and intermediary chordal forces from each PM were summed to examine if differences in cyclic tethering exist between each PM. For both PMs, significant differences in summed chordal forces were observed between the tested conditions (p<.001) (Table 3). For the posteromedial PM, summed forces were significantly greater than the control condition during IMR (p<.001) and each of the annuloplasty conditions (p<.001). Compared to IMR, summed forces on the posteromedial PM were observed to significantly decrease with oversized annuloplasty (p<.005), true-sized annuloplasty (p<.001), and undersized annuloplasty (p<.001).

Summed forces on the anterolateral PM were observed to significantly increase from the control condition to IMR (p<.001) and oversized annuloplasty (p<.05). Compared to IMR, summed forces were observed to statistically decrease at true and undersized annuloplasty (p<.05), respectively. While not reaching statistical significance, summed forces on the posteromedial PM were observed to be greater than those on the anterolateral PM at IMR and at each level of mitral annuloplasty.

Discussion

Computational tools exhibit significant potential for assessing how effective a proposed surgical strategy may be for addressing a patient's IMR MV anatomy and dysfunction. While advances in structural modeling and medical imaging have been made, modeling the

complex chordae tendineae remains challenging. To date, most MV models have relied on idealized chordal structures whose inter-study variation has been demonstrated to impact modeling results.[20,32] Compounding this uncertainty is the lack of experimental data providing boundary conditions for how the tethering of the chordae may change from IMR to UMA. Addressing both of these challenges is critical for improving IMR surgical planning tools and advancing their predictive capabilities.

Current best case scenarios utilize non-standard-of-care computed tomography (CT) imaging to generate high-resolution models of patient MV geometry and architecture.[32] The use of CT in this setting provides the ability to not only identify PM position but additionally demarcate major load bearing chordae that include the anterior strut and posterior intermediary chordae. Given CT may provide the best imaging modality to detail the MV's subvalvular structures, these models still require the appropriate boundary conditions to accurately predict the function and response of the chordae tendineae to both IMR and UMA.

This study was successful in generating an *in vitro* ground-truth data that may be used as boundary conditions for IMR computational models. This study was the first to simultaneously quantify leaflet coaptation, MR, anterior strut, and posterior intermediate chordal forces in the sequential transition from a healthy control, to IMR, and through multiple levels of undersized annuloplasty. As the algorithms and methods used in computational solvers can vary considerably, these data will aid the further development of computational tools to increase confidence in the simulated results. Additionally, these data reduce some uncertainty associated with extracting limited data from previous studies which may not directly represent IMR or UMA.

The presented data can enhance the modeling of idealized chordal structures within computational models (Figure 3). Computational models can assume a given chordal geometry and test the effect of IMR and or UMA under similar transmitral hemodynamics. The computationally observed values or trends for leaflet closure and chordal forces can be compared to the results herein to parametrically evaluate how the chosen chordal geometry influences coaptation and tethering. Based on these differences, the assumed chordal geometry can be iteratively tuned in both number and geometry to more accurately achieve a target coaptation, MR, and force distribution. With a more finely tuned chordal architecture, higher confidence will exist for subsequent simulations of progressive disease or surgical repairs. These evaluations may be best completed prior to the application of the developed methods to patient MV modeling.

Summed chordal forces from each PM were used to examine if differences in cyclic tethering exist between each PM. Early studies by Jensen et al. demonstrated PM displacement to increase the cyclic PM forces.[12] With inferior myocardial infarctions, the posterior papillary muscle is displaced more than the anterior papillary muscle.[3,5,6–8,30] As a result, the summation of the intermediary and strut chordal forces is expected to be greater for the posteromedial PM. When the summed forces between the PMs for each experimental condition were compared, no statistical differences were found (Table 3). This in part suggests that other chordae may be bearing additional loading whose tethering also likely contributes to leaflet malcoaptation. Understanding the tethering of other chordae, their relationship with strut chordal tethering, and their effect on coaptation in IMR and annuloplasty may lead to improved mitral valve repair techniques.[23,25]

Prior to this study, Nielsen et al. utilized a porcine model to evaluate the effect of acute IMR on marginal (also referred to in literature as primary) chordae tendineae forces for both PMs and leaflets.[23] For the anterolateral PM, anterior leaflet marginal chordal forces were

observed to statistically increase from control to IMR (p<.05) while non-significant decreases were observed in posterior marginal chordal forces. For the infarcted posteromedial PM, posterior leaflet marginal chordal forces remained relatively unchanged from control to IMR; however, anterior leaflet marginal chordal forces were significantly decreased (p<.05). One explanation for these changes in chordal forces is that mitral leaflet malcoaptation (due to restrictive posterior leaflet motion) reduces the posterior leaflet surface area exposed to the LV pressure. The authors' hypothesized this mechanism to reduce the chordal forces of the posterior leaflet and contribute to further mitral leaflet malcoaptation.[23]

In comparison to previous studies, the chordal forces reported herein are in good agreement with *in vitro* and large animal studies. For a healthy MV geometry, mean anterior leaflet strut and intermediary chordal forces have been found to range from approximately 0.65–1.22 N (Compared to 0.62–0.71 N in this study).[9,14,15,23,25] For the posterior leaflet, previous studies have reported a mean range of 0.25–0.78 N (Compared to 0.28–0.49 N in this study). [9,14,15,25] Compared to the forces in the study, the larger range of choral forces measured for a healthy MV geometry is attributed to the wide range of MV sizes used in previous studies. As the magnitude of chordal forces is directly related to the area of the MV leaflets exposed to the transvalvular pressure gradient, the greater the valve size, the larger the chordal force.[25]

While no previously published data exists for strut and intermediary chordal forces in IMR or UMA, an in vitro study has evaluated the effect of isolated papillary muscle displacement on strut and intermediary chordal tethering forces.[14] In the study, a parametric sweep of 5 mm displacements of both PMs in the apical, lateral, and posterior directions was performed. Significant increases in anterior strut and posterior intermediary chordal forces were observed when both PMs were displaced in either the apical or apical and lateral directions. Compared to the present study, these conditions most closely resemble a condition of true-sized annuloplasty. Our results compare favorably to that of Jimenez et al. by demonstrating anterior strut and posterior intermediary chordal forces significantly increase from the control condition with a true-sized annulus.[14] The results presented by Jimenez et al., Nielsen et al., and those herein provide complimentary information for how strut, intermediary, and marginal chordal tethering may be affected by either symmetric or asymmetric PM displacement towards the further development of computational MV models.[14,23]

Despite the advantages of the present study, there are limitations associated with the experimental methods. A3-P3 leaflet coaptation was not quantified due to the difficulty in imaging the thin and ill-coapting ovine leaflets. The described MV simulator can recreate the systolic geometric configuration of the mitral valve but at present does not incorporate the diastolic relaxation of the mitral annulus and systolic papillary muscle contraction. While in patients both the annular and papillary muscle dynamics may be ablated with the implantation of a complete rigid undersized annuloplasty ring and LV ischemia, the inclusion and intelligent variation of these parameters within the simulator would likely increase modeling accuracy.

Although only the anterior strut and posterior intermediate chordal forces were quantified, these chordae are known to bear the largest loads and have been demonstrated to most significantly contribute to leaflet malcoaptation in IMR.[25] With left ventricular dilatation and papillary muscle displacement, the strut and intermediary chordae tether the belly of each mitral leaflet and can lead to restricted leaflet motion, regional loss of coaptation, and MR.[2,3,8,30] Strut and intermediary chordae have additionally been implicated in UMA repair failure through long term post-operative left ventricular dilation, which further exacerbates

sub-valvular tethering.[11,17,21] For these reasons, these data can provide critical boundary conditions to further develop *in silico* platforms to model IMR and UMA.

In our study, IMR was modeled after a well-established ovine model of a chronic posteroinferior myocardial infarction.[7,30] Although myocardial infarcts vary in age, size, and location; posteroinferior ventricular infarcts exhibit a greater clinical prevalence and higher incidence of IMR.[16,19] A report by Gillinov et al. involving nearly 500 patients treated over 13 years at the Cleveland Clinic demonstrated 73% of patients had posterior wall motion abnormalities and 63% presented with abnormalities in inferior wall motion.[6,8] Although infarctions in locations other than the inferior side occurred, they were less common and likely represent the diffuse nature of coronary atherosclerosis that is present in most IMR patients.[8]

Conclusions

The present study provides for the first time a novel comprehensive data set for refining the ability of computational mitral valve models to simulate IMR and UMA. It is the first study to parametrically evaluate MV coaptation, MR, and strut and intermediary chordal forces in the sequential transition from a control to IMR and annuloplasty geometry. The quantification of these sequential effects is a significant finding and improves on the use of data from multiple studies whose materials and methods may not directly represent IMR or UMA.[25] This data is important for not only for improving computational modeling boundary conditions but also assessing modeling results. Combined with the results of previous studies, these data provide a ground-truth data set for the future development and refinement of MV computational models and future surgical planning tools.

Acknowledgments

Abbreviation, Symbols, and Terminology

ALPM	anterolateral papillary muscle
IMR	ischemic mitral regurgitation
MV	mitral valve
MR	mitral regurgitation
PM	papillary muscle
PMPM	posteromedial papillary muscle
UMA	undersized mitral annuloplasty

References

1. Badiwala MV, Verma S, Rao V. Surgical Management of Ischemic Mitral Regurgitation. Circulation. 2009; 120:1287–1293. [PubMed: 19786642]

2. Bolling SF, Pagani FD, Deeb GM, Bach DS. Intermediate-term outcome of mitral reconstruction in cardiomyopathy. The Journal of Thoracic and Cardiovascular Surgery. 1998; 115:381–388. [PubMed: 9475533]

3. Braun J, van de Veire NR, Klautz RJM, Versteegh M, Holman ER, Westenberg J, Boersma E, van der Wall EE, Bax JJ, Dion RAE. Restrictive mitral annuloplasty cures ischemic mitral regurgitation and heart failure. The Annals of Thoracic Surgery. 2008; 85:430–436. [PubMed: 18222238]

4. Burlina P, Sprouse C, Mukherjee R, DeMenthon D, Abraham T. Patient-Specific Mitral Valve Closure Prediction Using 3D Echocardiography. Ultrasound in Medicine & Biology. 201310.1016/j.ultrasmedbio.2012.11.009

5. Carpentier, A.; Adams, DH.; Filsoufi, F. Carpentier's Reconstructive Valve Surgery. Saunders; Maryland Heights, Missouri: 2010.

6. Gillinov AM, Wierup PN, Blackstone EH, Bishay ES, Cosgrove DM, White J, Lytle BW, McCarthy PM. Is repair preferable to replacement for ischemic mitral regurgitation? The Journal of Thoracic and Cardiovascular Surgery. 2001; 122:1125–1141. [PubMed: 11726887]

7. Gorman JH III, Gorman RC, Jackson BM, Enomoto Y, St John-Sutton MG, Edmunds LH Jr. Annuloplasty ring selection for chronic ischemic mitral regurgitation: lessons from the ovine model. The Annals of Thoracic Surgery. 2003; 76:1556–1563. [PubMed: 14602285]

8. Gorman, RC.; Gorman, JH., III; Edmunds, H, Jr. Ischemic Mitral Regurgitation, in Cardiac surgery in the adult. Cohn, LH.; Henry Edmunds, JL., editors. McGraw-Hill; New York, NY: 2003. p. 751-769.

9. Granier M, Jensen MO, Honge JL, Bel A, Menasché P, Nielsen SL, Carpentier A, Levine RA, Hagège AA. Consequences of Mitral Valve Prolapse on Chordal Tension: Ex Vivo and in Vivo Studies in Large Animal Models. The Journal of Thoracic and Cardiovascular Surgery. 2011; 142:1585–1587. [PubMed: 21955468]

10. He Z, Ritchie J, Grashow JS, Sacks MS, Yoganathan AP. In Vitro Dynamic Strain Behavior of the Mitral Valve Posterior Leaflet. Journal of Biomechanical Engineering. 2005; 127:504–511. [PubMed: 16060357]

11. Hung J, Papakostas L, Tahta SA. Mechanism of recurrent ischemic mitral regurgitation after annuloplasty: continued LV remodeling as a moving target. Circulation. 2004; 110:II85–II90. [PubMed: 15364844]

12. Jensen MO, Fontaine AA, Yoganathan AP. Improved In Vitro Quantification of the Force Exerted by the Papillary Muscle on the Left Ventricular Wall: Three-Dimensional Force Vector Measurement System. Annals of Biomedical Engineering. 2001; 29:406–413. [PubMed: 11400721]

13. Jensen H, Jensen MO, Smerup MH, Ringgaard S, Anderson NT, Wierup P, Hasenkam JM, Nielsen SL. Does down-sized ring annuloplasty induce papillary muscle relocation in ischemic mitral regurgitation? Journal of Heart Valve Disease. 2010; 19:692–700. [PubMed: 21214091]

14. Jimenez JH, Soerensen DD, He Z, Ritchie J, Yoganathan AP. Effects of papillary muscle position on chordal force distribution: an in-vitro study. Journal of Heart Valve Disease. 2005; 14:295–302. [PubMed: 15974521]

15. Jimenez JH, Soerensen DD, He Z, He S, Yoganathan AP. Effects of a saddle shaped annulus on mitral valve function and chordal force distribution: an in vitro study. Annals of Biomedical Engineering. 2003; 31:1171–1181. [PubMed: 14649491]

16. Kumanohoso T, Otsuji Y, Yoshifuku S, Matsukida K, Koriyama C, Kisanuki A, Minagoe S, Levine RA, Tei C. Mechanism of higher incidence of ischemic mitral regurgitation in patients with inferior myocardial infarction: Quantitative analysis of left ventricular and mitral valve geometry in 103 patients with prior myocardial infarction. Journal of Thoracic and Cardiovascular Surgery. 2003; 125:135–143. [PubMed: 12538997]

17. Kuwahara E, Otsuji Y, Iguro Y, Ueno T, Zhu F, Mizukami N, Kubota K, Nakashiki K, Yuasa T, Yu B, Uemura T, Takasaki K, Miyata M, Hamasaki S, Kisanuki A. Mechanism of Recurrent/Persistant Ischemic/Functional Mitral Regurgitation in the Chronic Phase after Surgical Annuloplasty. Circulation. 2006; 114:I229–I534.

18. Lau KD, Diaz V, Scrambler P, Burriesci G. Mitral valve dynamics in structural and fluid-structure interaction models. Medical Engineering Physics. 2010; 32:1057–1064. [PubMed: 20702128]

19. Lung B. Management of ischaemic mitral regurgitation. Heart. 2003; 89:459–464. [PubMed: 12639884]

20. Mansi T, Voight I, Mengue A, Ionasec RI, Georgescu B, Noack T, Seeburger J, Comaniciu D. Towards Patient-Specific Finite-Element Simulation of MitraClip Procedure. Medical Image Computing and Computer-Assisted Intervention-MICCAI. 2011; 6891:452–459.

21. McGee EC, Gillinov AM, Blackstone EH. Recurrent mitral regurgitation after annuloplasty for functional ischemic mitral regurgitation. Journal of Thoracic and Cardiovascular Surgery. 2004; 128:916–924. [PubMed: 15573077]

22. Nielsen SL, Nygaard H, Fontaine AA, Hasenkam JM, He S, Andersen NT, Yoganathan AP. Chordal force distribution determines systolic mitral leaflet configuration and severity of functional mitral regurgitation. Journal of the American College of Cardiology. 1999; 33:843–853. [PubMed: 10080490]

23. Nielsen SL, Hansen SB, Nielsen KO, Nygaard H, Paulsen PK, Hasenkam JM. Imbalanced chordal force distribution causes acute ischemic mitral regurgitation: Mechanistic insights from chordae tendineae force measurements in pigs. Journal of Thoracic and Cardiovascular Surgery. 2005; 129:525–531. [PubMed: 15746734]

24. Pouch AM, Xu C, Yushkevich PA, Jassar AS, Vergnat M, Gorman JH III, Gorman RC, Sehgal CM, Jackson BM. Semi-automated mitral valve morphometry and computational stress analysis using 3D ultrasound. Journal of Biomechanics. 2012; 45:903–907. [PubMed: 22281408]

25. Rabbah JPM, Saikrishnan N, Siefert AW, Santhanakrishnan A, Yoganathan AP. Mechanics of Healthy and Functionally Diseased Mitral Valves: A Critical Review. Journal of Biomechanical Engineering. 201310.1115/1.4023238

26. Rim Y, McPherson DD, Chandran KB, Kim H. The effect of patient-specific annular motion on dynamic simulation of mitral valve function. Journal of Biomechanics. 201310.1016/j.jbiomech. 2013.01.014

27. Sacks MS, He Z, Baijens L, Wanant S, Shah P, Sugimoto H, Yoganathan AP. Surface strains in the anterior leaflet of the functioning mitral valve. Annals of Biomedical Engineering. 2002; 30:1281–1290. [PubMed: 12540204]

28. Siefert AW, Rabbah JPM, Koomalsingh KJ, Touchton SA Jr, Saikrishnan N, McGarvey JR, Gorman RC, Gorman JH III, Yoganathan AP. In-Vitro Mitral Valve Simulator Mimics Systolic Valvular Function of Chronic Ischemic Mitral Regurgitation Ovine Model. The Annals of Thoracic Surgery. 2013; 95:825–830. [PubMed: 23374445]

29. Stevanella MF, Maffessanti CA, Conti E, Votta A, Arnoldi M, Lombardi PO, Caiani EG, Redaelli A. Mitral valve patient specific finite element modeling from cardiac MRI: application to an annuuloplasty procedure. Cardiovascular Engineering and Technology. 2011; 2:66–76.

30. Tibayan FA, Rodriguez F, Zasio MK, Bailey L, Liang D, Daughters GT, Langer F, Ingels NB Jr, Miller DC. Geometric Distortions of the Mitral Valvular-Ventricular Complex in Chronic Ischemic Mitral Regurgitation. Circulation. 2003; 108:II-116–II-121. [PubMed: 12970219]

31. Votta E, Maisano F, Bolling SF, Alfieri O, Montevecchi FM, Redaelli A. The Geoform Disease-Specific Annuloplasty System: A Finite Element Study. The Annals of Thoracic Surgery. 2007; 84:92–101. [PubMed: 17588392]

32. Wang Q, Sun W. Finite element modeling of mitral valve dynamic deformation using patient-specific multi-slices computed tomography scans. Annals of Biomedical Engineering. 2013; 41:142–153. [PubMed: 22805982]

33. Wenk JF, Zhang Z, Cheng G, Malhotra D, Acevendo-Bolton G, Burger M, Suzuki T, Soloner DA, Wallace AW, Guccione JM, Ratcliffe MB. First finite element model of the left ventricle with mitral valve: insights into ischemic mitral regurgitation. The Annals of Thoracic Surgery. 2010; 89:1546–1553. [PubMed: 20417775]

34. Wong VM, Wenk JF, Zhang Z, Cheng G, Acevedo-Bolton G, Burger M, Saloner DA, Wallace AW, Guccione JM, Ratcliffe MB, Ge L. The Effect of Mitral Annuloplasty Shape in Ischemic Mitral Regurgitation: A Finite Element Simulation. The Annals of Thoracic Surgery. 2012; 93:776–782. [PubMed: 22245588]
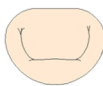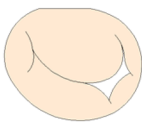
FIGURE 1.
Summary of experimental conditions progressing from control to ischemic mitral regurgiation (IMR), oversized mitral annuloplasty, true-sized mitral annuloplasty, and undersized mitral annuloplasty (UMA). (Please note images are not drawn to scale)
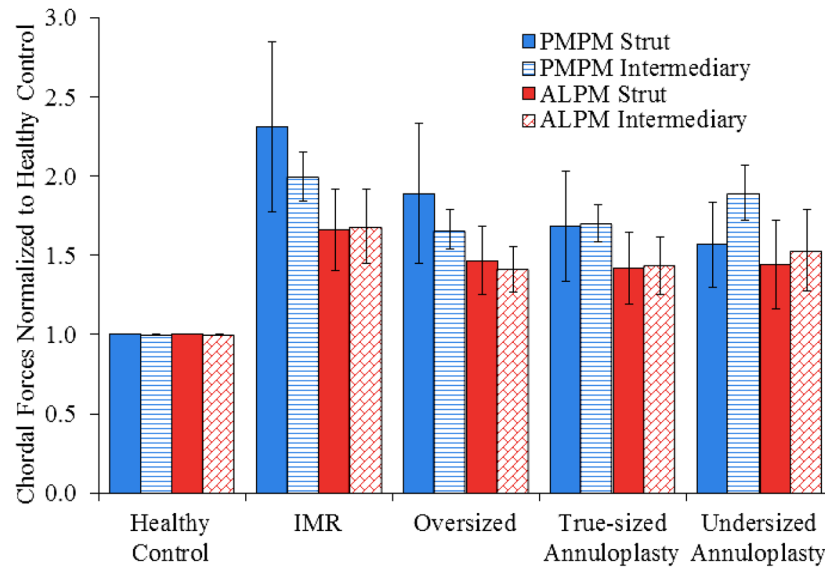
FIGURE 2.
Chordal forces from the posteromedial papillary muscle (PMPM) and anterolateral papillary muscle (ALPM) were normalized to the forces observed during the healthy control condition to demonstrate relative changes in cyclic chordal tethering with ischemic mitral regurgitation (IMR) and increasing degrees of annular under sizing.
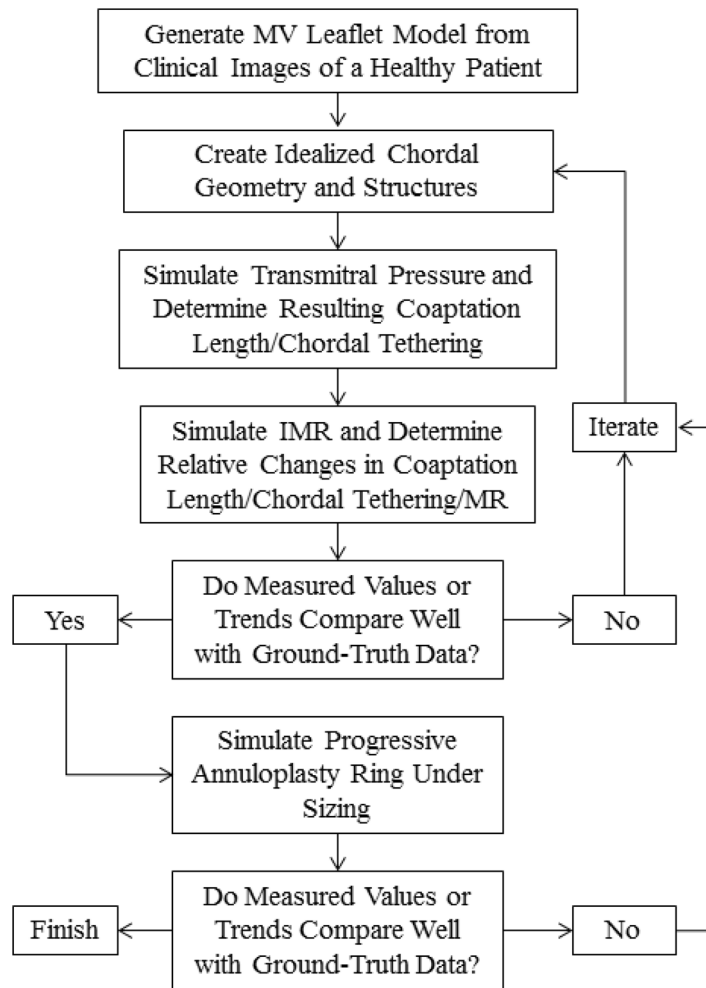
FIGURE 3.
Example iterative scheme for improving modeling of idealized chordal structures and geometry with the results of this study

TABLE 1

Effect of the evaluated conditions on mitral regurgitation volume (MRV) and A2-P2 coaptation length (CL); asterisks (*) and dagger (†) denote significant differences relative to the healthy control condition and ischemic mitral regurgitation condition, respectively.

Measurement	Healthy Control	Ischemic Mitral Regurgitation	Oversized Annuloplasty	True-Sized Annuloplasty	Undersized Annuloplasty
MRV [mL]	27.6 ± 1.4	47.0 ± 2.2 *	37.4 ± 2.2 * †	27.5 ± 1.2 †	24.9 ± 1.2 †
CL [mm]	4.84 ± 0.13	3.19 ± 0.14 *	3.54 ± 0.11 *	3.90 ± 0.13 †	4.75 ± 0.16 †

TABLE 2

Effect of the evaluated conditions on anterior strut (AS) and posterior intermediary (PI) chordal forces (mean ± standard error) originating from the posteromedial (PM) and anterolateral (AL) papillary muscles; asterisks (*) and dagger (†) denote significant differences relative to the healthy control condition and ischemic mitral regurgitation condition, respectively.

Papillary Muscle	Chordae Tendineae	Healthy Control	Ischemic Mitral Regurgitation	Oversized Annuloplasty	True-sized Annuloplasty	Undersized Annuloplasty
PM	AS	0.71 ± 0.08	1.23 ± 0.11 *	0.99 ± 0.10 * †	0.91 ± 0.09 * †	0.88 ± 0.08 * †
	PI	0.28 ± 0.03	0.55 ± 0.08 *	0.47 ± 0.07 *	0.47 ± 0.06 *	0.51 ± 0.07 *
AL	AS	0.62 ± 0.11	0.80 ± 0.14 *	0.72 ± 0.12	0.68 ± 0.11	0.66 ± 0.10 †
	PI	0.49 ± 0.09	0.71 ± 0.13 *	0.61 ± 0.11	0.55 ± 0.09 †	0.53 ± 0.09 †

TABLE 3

Effect of the evaluated conditions on strut and intermediary chordal forces summed by papillary muscle; asterisks (*) and dagger (†) denote significant differences relative to the healthy control condition and ischemic mitral regurgitation condition, respectively.

Papillary Muscle	Healthy Control	Ischemic Mitral Regurgitation	Oversized Annuloplasty	True-sized Annuloplasty	Undersized Annuloplasty
Posteromedial	0.98 ± 0.08	1.76 ± 0.11 *	1.50 ± 0.10 *†	1.41 ± 0.09 *†	1.42 ± 0.11 *†
Anterolateral	1.01 ± 0.12	1.41 ± 0.19 *	1.24 ± 0.18 *	1.18 ± 0.16 †	1.14 ± 0.14 †